

Primary Liver Cells Cultured on Carbon Nanotube Substrates for Liver Tissue Engineering and Drug Discovery Applications

Che Azurhanim Che Abdullah,^{*,†,‡} Chihye Lewis Azad,^{||} Raquel Ovalle-Robles,^{||} Shaoli Fang,^{||} Marcio D. Lima,^{||} Xavier Lepró,^{||} Steve Collins,^{||} Ray H. Baughman,^{||} Alan B. Dalton,[†] Nick J. Plant,[§] and Richard P. Sear[‡]

[†]Department of Physics, Faculty of Science, University of Putra Malaysia, Serdang, Selangor 43300, Malaysia

[‡]Department of Physics, University of Surrey, Guildford, Surrey GU2 7XH, United Kingdom

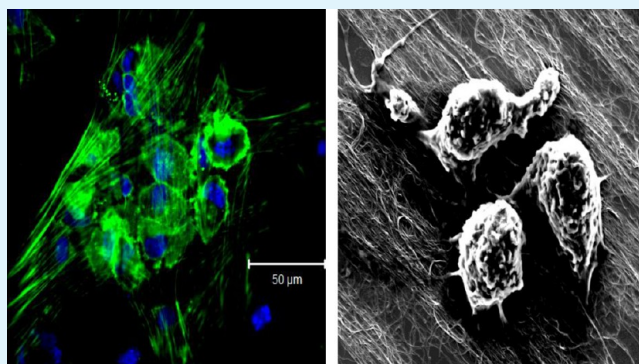
[§]Centre for Toxicology, Department of Biochemistry and Physiology, Faculty of Health and Medical Sciences, University of Surrey, Guildford, Surrey GU2 7XH, United Kingdom

^{||}The Alan G MacDiarmid NanoTech Institute, The University of Texas at Dallas, Richardson, Texas 75080-3021, United States

Supporting Information

ABSTRACT: Here, we explore the use of two- and three-dimensional scaffolds of multiwalled-carbon nanotubes (MWNTs) for hepatocyte cell culture. Our objective is to study the use of these scaffolds in liver tissue engineering and drug discovery. In our experiments, primary rat hepatocytes, the parenchymal (main functional) cell type in the liver, were cultured on aligned nanogrooved MWNT sheets, MWNT yarns, or standard 2-dimensional culture conditions as a control. We find comparable cell viability between all three culture conditions but enhanced production of the hepatocyte-specific marker albumin for cells cultured on MWNTs. The basal activity of two clinically relevant cytochrome P450 enzymes, CYP1A2 and CYP3A4, are similar on all substrates, but we find enhanced induction of CYP1A2 for cells on the MWNT sheets. Our data thus supports the use of these substrates for applications including tissue engineering and enhancing liver-specific functions, as well as in *in vitro* model systems with enhanced predictive capability in drug discovery and development.

KEYWORDS: carbon nanotubes, tissue engineering, liver toxicity testing, rat hepatocytes, albumin, CYP enzyme activities



1. INTRODUCTION

Improved *in vitro* model systems for studying drug metabolism and toxicity testing are urgently needed for faster, cheaper, and safer drug development, with reduced testing on animals. This is particularly true for the liver, the major organ of drug metabolism in the body. Liver toxicity (hepatotoxicity) is responsible for a high percentage of late-stage attrition in drug development and on-market withdrawals.^{1,2} A number of liver models have been proposed, ranging from computational,^{3,4} through liver slices,⁵ to cultures of primary or secondary liver cells.⁶ Cultured primary hepatocytes are currently seen as the gold-standard for drug testing, but it is acknowledged that they rapidly alter their phenotype in culture, meaning that screening assays must be carefully validated, and complicates extrapolation to *in vivo*.^{7,8} In addition, their limited life in culture (approximately 1 week) and varied sourcing of human primary cells further complicates their use at an industrial scale. It is therefore imperative to develop novel approaches that either increase the predictive power of primary hepatocytes, increase their survival in culture, or preferably both.

Various approaches have been taken to try and improve the utility of hepatocytes for drug development. Hepatocyte cells cultured in a conventional monolayer culture do show liver-specific activity but they rapidly lose liver-specific enzyme activity and fail to form the cellular polarization required for the correct functioning of membrane-bound drug transporters.^{7,9} Both these issues can be resolved to some extent through the use of advanced culture methodologies such as sandwich culture, where cells are grown between layers of, for example, collagen. Primary hepatocytes cultured in sandwich configuration demonstrate improved maintenance of hepatocyte-specific functions such as morphology (polynucleation, polarized phenotype, and functional bile canicular network), albumin secretion, intrinsic metabolism (glycogen storage, lipid metabolism, and urea synthesis), and drug metabolizing and transport functions.^{9–11}

Received: March 28, 2014

Accepted: May 30, 2014

Published: June 16, 2014

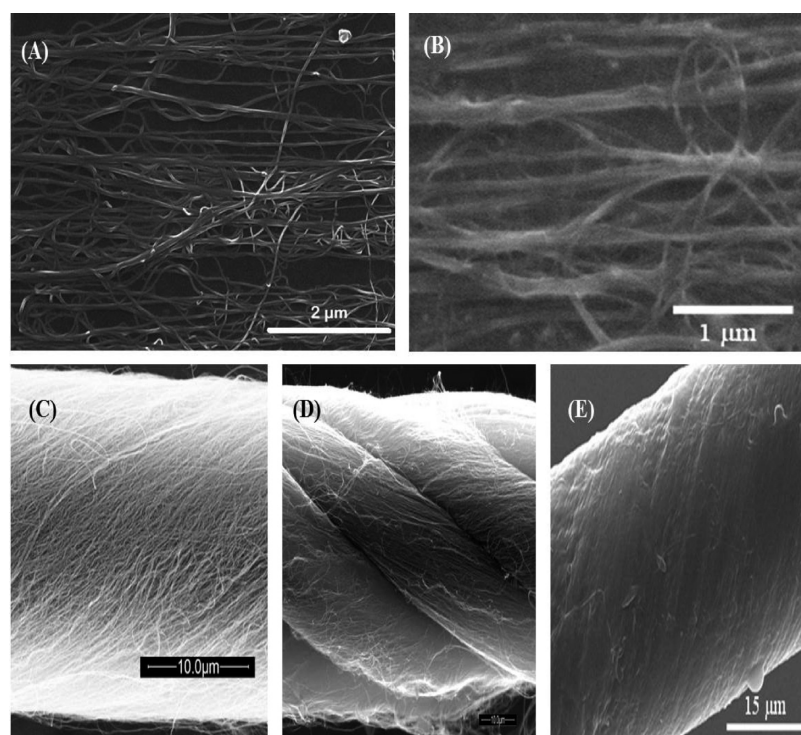


Figure 1. SEM images showing topography of the aligned sheet (2D) and yarn (3D) substrates, before and after coating with collagen solution. MWNT sheet (A), single-ply yarn (C), and 6-ply yarn (D), all without collagen coating. The aligned MWNT sheet (B) and single-ply MWNT yarn (E) are after collagen coating.

The physiological underpinning for the improved *in vivo*-like phenotype of primary hepatocytes cultured in sandwich culture is that, in the body, cells are surrounded by and interact with a complex three-dimensional extracellular matrix (ECM). The ECM contains nanoscale structures such as the collagen helix, which is approximately 1.5 nm across, and provides physical cues that affect cell behavior and hence the formation of functional tissues from cells. In sandwich culture systems, both natural and artificial matrices are used to mimic these structures. However, it is important to note that the ECM is more complex than a simple collagen matrix, both in terms of its content and its controlled 3D topography. It is known that these microscale topographies and patterns influence cellular behavior for many cell types,^{12–14} and this presents the possibility of improved matrices that mimic the ECM more closely and thus improve hepatocyte phenotypic behavior. Materials with controlled nanoscale topography such as carbon nanotubes (CNTs) represent ideal materials for the creation of such optimized ECM mimics.

The potential utility of improved ECM replacements has been explored previously by others: For example, Zhang et al. cultured hepatocytes in a sandwich between a porous silicon nitride membrane conjugated with galactose (top) and a polyethylene terephthalate (PET) film (bottom), demonstrating improved differentiated functions compared to cells in a collagen sandwich.¹⁵ Also, Wang et al. investigated hepatocytes cultured on PuraMatrix scaffold, a synthetic peptide that can self-assemble into three-dimensional interweaving nanofiber scaffolds to form a hydrogel.¹⁶ The hepatocytes formed spheroids on the PuraMatrix and demonstrated higher albumin and urea secretion and cytochrome P450 (CYP1A1) activity than cells in the collagen sandwich. Recently, Rothenberg and co-workers studied nanofiber surfaces (Ultra-Web and Ultra-

Web polyamines) and demonstrated enhanced cytochrome P450 (CYP3A) activity, with respect to cells on collagen surfaces.¹⁷ Following induction with dexamethasone (Dex) and pregnenolone-16 α -carbonitrile (PCN), CYP3A activity measured for hepatocytes on Ultra-Web surfaces was 5-fold higher than hepatocytes grown on collagen.

CNTs have a number of potential advantages as the active materials in optimized matrices for cell growth. They are inert, mechanically robust, and electrically conductive and provide a nanoscale, tunable fibrous topography to any surface they create or are deposited upon. Importantly, CNTs are biocompatible materials with great potential as cell-supporting substrates in tissue engineering, where substrates play an important role in the tissue development process. CNTs offer high mechanical strength, can be easily functionalized, and can provide the structural reinforcement for tissue scaffolding. In addition, the nanotopographic characteristic of both multi-walled-carbon nanotubes (MWNTs) sheets and yarns are on the same length scale as that of the ECM found in intact tissues, and the MWNTs are aligned, as the collagen fibers of the ECM can be.¹⁸

Tsai and Lin revealed the impact of nanopatterned topography on hepatocyte morphology and functions.¹⁹ The morphology of HepG2/C3A hepatoma cells was dramatically different on their nanogrooved substrates, being elongated and aligned along the nanogrooves in comparison to cells on flat substrates. Hepatocyte-specific functions, albumin secretion, and urea conversion were analyzed quantitatively and found to be enhanced on nanogrooved substrates with a shallow depth.

Cell functions can be modulated by culturing cells on synthetic materials with controlled nanoscale topography mimicking the ECM.²⁰ CNT-based substrates such as MWNTs can serve as synthetic ECM for cell culture *in vitro*.

So far, no papers reported the use of CNT-based substrates for applications to liver tissue engineering.

In this paper, we present results for the effect of MWNT substrates on primary liver cell behavior including adhesion, morphology, and proliferation as well as liver-specific functional activities such as albumin synthesis, polarization, and the expression of clinically important enzyme activities, cytochrome P450 CYP1A2 and CYP3A4.

2. MATERIALS AND METHODS

2.1. Preparation of Aligned MWNT Sheets. The nanotube sheets were drawn from a sidewall of MWNT forests, which were synthesized by catalytic chemical vapor deposition, using acetylene gas as the carbon source.^{21,22} Thermogravimetric analysis (TGA) data shows that the MWNTs used had approximately 3 wt % catalytic contaminants. The diameter of the MWNTs was approximately 10 nm, and the forest heights averaged 185 μm . Fibril branching within the forest enables the sheet drawing process, making a laterally interconnected fibril network.²¹ These aerogel sheets are ultralight, transparent, and electrically conductive, having a mass per unit area density of 1–3 $\mu\text{g}/\text{cm}^2$.²¹ The MWNT sheets are highly aligned; Zhang et al.²¹ applied Raman spectroscopy and reported a polarization degree of between 0.69 and 0.75.

The aerogel sheets were then applied to a cover glass. During the application process, the sheets were densified with 2-propanol along the alignment of the nanotubes and allowed to air-dry. The procedure also introduces some variation in the local density of the MWNT sheet. This nonuniformity can be seen in the SEM images of our sheets, Figure 1A,B, where darker curves represent larger and denser MWNT bundles. It should also be borne in mind that whenever a liquid is applied to the substrate (e.g., when cells are added) movement of the MWNT bundles occurs due to the fact that the bundles are not bonded to the glass. In addition to the aligned MWNT sheets, we also prepared 3D MWNT substrates called yarns.

2.2. Preparation of MWNT Yarns. The MWNT yarn was fabricated by introducing a twist during sheet draw from the nanotube forests to make a single-ply yarn. Multiply yarns were prepared by twisting multiple single-ply yarns around each other.²³ The yarns used in these experiments were not functionalized or chemically treated. Free standing yarns were placed horizontally onto a custom designed experimental fixture made of polydimethylsiloxane (PDMS; Slygard 184, Dow Corning).

The topographies of MWNT yarns were characterized using SEM (Hitachi S4000), as shown in Figure 1. Studies of the changes in topography of both aligned MWNT sheets and yarns following coating with collagen solution were also carried out using SEM.

Both MWNT sheets and yarns were sterilized by immersion in 70% ethanol (ETOH) for 5 min and then allowed to air-dry in a sterile culture hood. Prepared substrates were then exposed to ultraviolet (UV) light for 30 min to sterilize them before use in cell experiments.

2.3. Collagen Coated Substrates. Control (plain cover glass) and test (MWNT sheets on cover glass) substrates placed in 6-well plates were precoated with rat tail tendon collagen (Sigma-Aldrich, Cat No. C3867) solution (1 mg/mL) overnight at 4 °C and kept on ice. Prior to cell seeding, substrates were washed with PBS followed by culture medium. Finally, a cell suspension at a concentration of 1×10^6 cells per mL was added to each well and incubated at 37 °C.

In the case of the sandwich culture configuration, following overnight incubation to allow cell attachment, both culture medium and unattached cells were removed and a second layer of collagen solution (1 mg/mL) was overlaid on the top of the culture for an additional 8 h. After that, 2 mL of prewarmed culture medium was added on top of the second layer collagen gel, and then, the medium was changed on a daily basis until the culturing was over.

2.4. Cell Culture. Plateable, cryopreserved primary rat hepatocytes (from male Sprague–Dawley rats; Lot No: Rs619 and Rs660) were purchased from Invitrogen (Paisley, UK). These primary cells were cultured in the standard way, as described in the Supporting Information. Cells were first checked for viability (70% to 90% viable)

and then seeded (1×10^6 cells per mL) on test and control substrates precoated with collagen Type I solution.

For details of the culture of these cells, see the Supporting Information. Cells were seeded on test and control substrates at a density of 5×10^4 cells per mL in the case of aligned MWNT sheets and a glass coverslip and at 5×10^5 cells per mL for MWNT yarns. The Supporting Information also contains details of our standard methods for fixing and fluorescent staining of F-actin, albumin, and the nuclei of cells on our substrates.

2.5. Microscopy and Image Acquisition. Confocal imaging was conducted using a Zeiss LSM 510 META laser scanning confocal microscope. AlexaFluor phalloidin (actin stain) and albumin stained with an antialbumin antibody using a FITC labeled secondary antibody were excited with the argon laser line of 488 nm and DRAQ5 (nucleus counterstain) with the helium–neon laser line of 633 nm. The emission signals passed through the 505–530 nm and 649–799 nm filters, respectively.

All images were captured using either the plan-neofluar 10 \times air or 40 \times oil objectives, or the plan-apochromat 20 \times air and 63 \times oil objectives, and collected in multichannel mode. A multitrack configuration was used in order to minimize any bleed-through effect from the different channels. Pinholes were set at 1 Airy unit (AU), which corresponds to an optical slice of 0.8 μm for both channels. All confocal data sets were of frame size 512 by 512 pixels, scan zoom of 1, and line averaged four times. All images were processed by using the Zeiss LSM browser and ImageJ software from National Institutes of Health (NIH). We also took images of cells grown on both control and test substrates using a phase contrast mode of the Nikon Eclipse TS 100 light microscope.

2.6. Scanning Electron Microscopy and Image Acquisition. Cells on collagen coated substrates, which have been dehydrated through an ethanol/water series (30%, 50%, 70%, 85%, 95%, and 100%), were allowed to dry for a few hours before being mounted on aluminum stubs using Araldite glue and left overnight prior to being sputter coated. For further details of the fixing procedure, see the Supporting Information.

Samples were sputter coated with a 2–5 nm layer of gold–palladium mixture for 2 min in a partial pressure of argon atmosphere using the Emitech K575X Peltier cooled sputter coater. Samples were imaged using a field emission SEM (Hitachi S-4000). The secondary electron detector was used to image the samples. The surface topography of both scaffolds and the cells on the scaffolds were visualized at an accelerating voltage in the range of 10 to 15 kV.

2.7. Liver Function Assays. We performed XTT cell proliferation, MRP2 drug transporter efflux, Cytochrome-P450 activity, and ELISA assays. In all cases, we followed standard procedures, which are described in the Supporting Information.

2.8. Statistical Analysis. Experiments were undertaken on at least two independent occasions, with duplicate samples within each sample for assessment of technical variation. Data are expressed as the mean \pm standard deviation. Statistical analyses were performed using GraphPad Prism 5.0 (GraphPad Software). In the case of qualitative results (based on images), at least four representative images were taken from multiple samples for each condition.

3. RESULTS AND DISCUSSION

3.1. Substrate Characterization. We use two types of MWNT as substrates: 2D aligned MWNT sheets and 3D MWNT yarns. The physical and chemical properties of aligned sheets were characterized by AFM (tapping mode), SEM, and contact angle measurement as reported in our previous paper.²⁴ The root-mean-square (RMS) roughness of the densified MWNT sheets was 51 nm. The contact angle of water droplets was $73 \pm 5^\circ$ (mean \pm standard deviation of 3 measurements). The lower contact angle of the aligned MWNT substrate, lower than either graphite or entangled CNTs, is due to the interaction of water with the (hydrophilic) glass underneath the MWNT sheets.²⁵

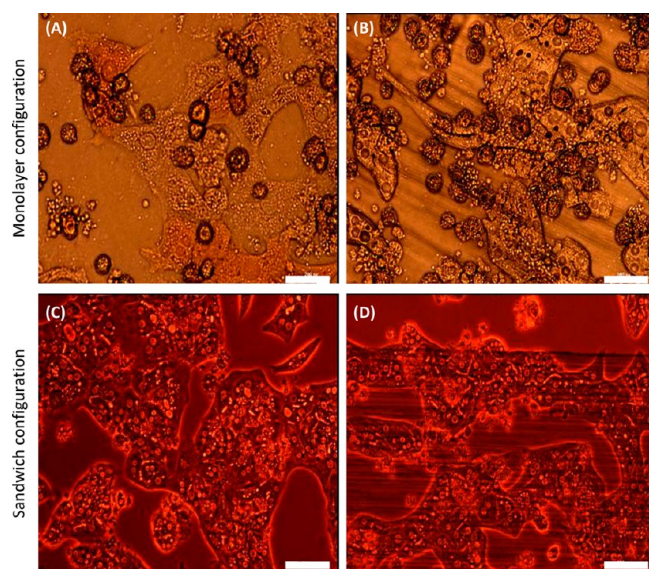


Figure 2. Morphology of primary rat hepatocytes plated in monolayer and sandwich culture configurations, observed using phase contrast microscopy. Phase contrast micrographs of hepatocytes in monolayer configuration on: (A) a glass coverslip and (B) aligned MWNTs. The phase contrast micrographs of rat hepatocytes in sandwich culture (overlaid with a second layer of collagen) on (C) a glass coverslip and (D) aligned MWNTs. Scale bar is 200 μm . (A) and (B) were taken using 20 \times magnification while (C) and (D) were taken using 10 \times magnification.

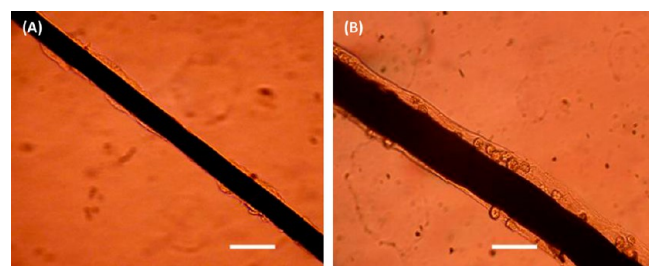


Figure 3. Optical micrographs showing primary rat hepatocytes grown on 3D MWNT yarns in sandwich culture configuration observed using phase contrast microscopy. Phase microscopy of hepatocytes on (A) single-ply yarn and (B) 6-ply yarn. Note that the cells are on the surface of yarns that are tens of micrometers thick, and so, some visible cells are in focus but others are out of focus. Scale bar is 50 μm .

MWNT yarns are prepared via twist spinning of the MWNT sheet strip from a MWNT forest. Multi-ply yarns are created by introducing a twist of more-than-one-ply MWNT yarn. Figure 1 contains images of aligned MWNT sheets and images showing yarn topography before and after coating with rat-tail collagen. The average diameter of single-ply and 6-ply yarns was determined using SEM and image analysis and was found to be 27 ± 3 and 68 ± 9 μm , respectively (mean \pm standard deviation of 3 measurements).

3.2. Cellular Morphology of Primary Rat Hepatocyte (PRH) on 2D and 3D Substrates with Nanoscale Topography. We cultured and studied primary rat hepatocytes on our substrates. The hepatocytes are polygonal in shape, and their nuclei show distinct nucleoli. The majority of hepatocytes are mononucleated (single nuclei) but some were bi- or multinucleated. The exact biological rationale underlying hepatocyte nucleation and ploidy status is controversial, but it is clear that this is an important feature of their normal biological

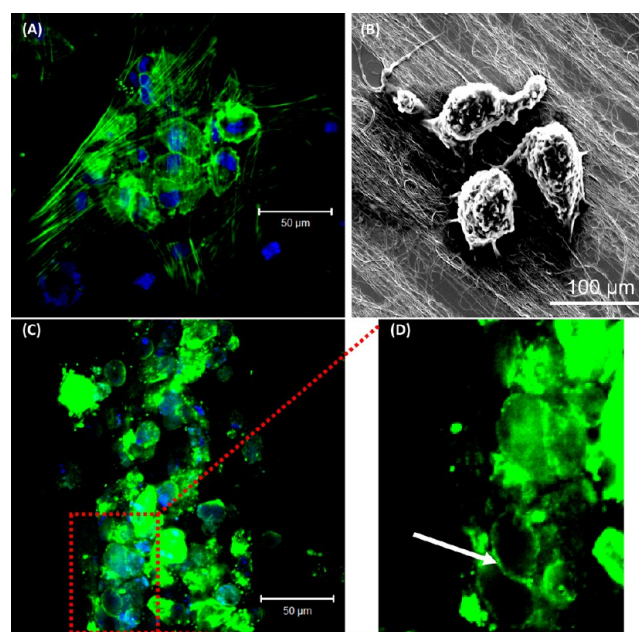


Figure 4. Representative images showing the arrangement of the F-actin cytoskeleton (indicated by green fluorescence staining) in primary rat hepatocytes cultured in different configurations on aligned MWNTs. (A) is for monolayer culture and (C) is for sandwich culture of rat hepatocytes. Nuclei are stained with DRAQS (blue). The SEM image (B) shows the typical shape of rat hepatocytes in sandwich culture. The close up image (D) shows the cortical actin distribution, predominantly in the periphery of the cell including at regions of cell–cell contact.

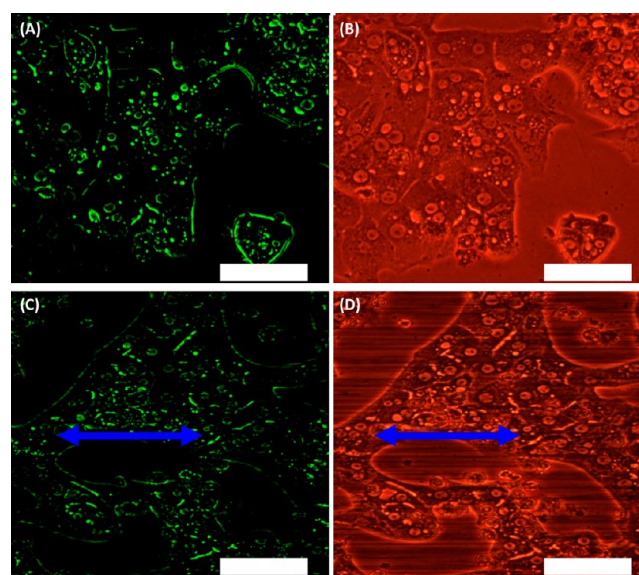


Figure 5. Representative images indicating retention of CDF in the bile canaliculi of sandwich-cultured rat hepatocytes after 5 days in culture. Sandwich-cultured hepatocytes on both aligned MWNT sheets and flat glass coverslips were incubated with CDFDA (10 μM) in standard buffer for 30 min. The upper images are of hepatocytes on coverslips, and the lower images are of hepatocytes on aligned MWNT sheets. The accumulation of CDF in the bile canaliculi is shown via fluorescence microscopy in (A) and (C); CDF is shown as green. The morphology of hepatocytes is observed using phase contrast mode optical microscopy in (B) and (D). Scale bars are 200 μm . The direction of the MWNT grooves is indicated by the blue arrow in the image.

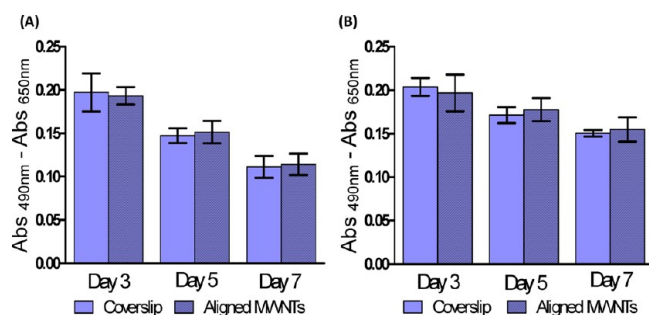


Figure 6. Graphs showing hepatocyte viability over 7 days in culture. The viability of hepatocytes (A) in monolayer configuration and (B) in sandwich culture configuration was assessed using the XTT assay. Data are obtained after 3, 5, and 7 days postplating. Each viability is the mean and standard deviations of 3 measurements. In all cases, the error bars for coverslip and MWNT sheet measurements overlap.

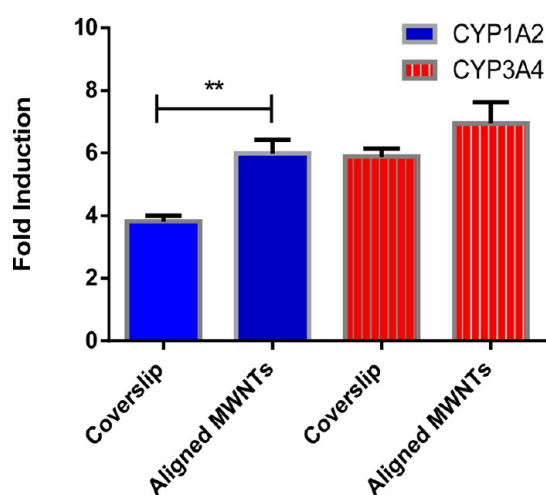


Figure 7. Effect of substrate topography on the induction of CYP1A2 and CYP3A4 activity, of primary rat hepatocytes in sandwich configuration after 5 days of culture. CYP1A2 enzyme expression was induced with 10 μ M beta-Naphthoflavone (β -NF), while CYP3A4 expression levels were induced with 10 μ M dexamethasone (Dex); in both cases, the induction period was 48 h. Enzyme activity was then measured for the mean obtained from two samples (aligned MWNT sheets or coverslips) from three independent experiments, for both induced and control samples; i.e., each point is the mean (\pm standard deviation) of 6 samples. Two asterisks indicate that, according to an unpaired two-tailed *t* test, the fold CYP1A2 induction is significantly ($P = 0.0014$) different (higher) on our aligned MWNTs than on coverslips.

functioning.^{26,27} Here, we study quantitatively the behavior of primary rat hepatocytes on surfaces with nanoscale topography; in particular, we quantify CYP450 activity and albumin secretion.

We cultured primary rat hepatocytes on our aligned MWNT sheet substrates and control substrates (glass coverslips) precoated with collagen Type 1. It is known that the survival of hepatocytes *in vitro* can be increased if they are cultured on substrates or scaffolds precoated with an ECM adhesion protein, particularly collagen Type 1.²⁸ This can be done in two ways: The first is a monolayer configuration, where the cells are on a collagen-coated surface. The second is a sandwich configuration, where hepatocytes are between thin layers of collagen. The optical images in Figure 2 show the morphology of primary hepatocytes cultured in monolayer (top panel) and

sandwich culture (bottom panel). The hepatocytes are on aligned MWNT sheets (Figure 2B,D) and on control glass coverslips (Figure 2A,C). Hepatocytes in sandwich culture configuration are both mono- and binucleated, while the majority of hepatocytes in monolayer culture are binucleated.

We have also made preliminary studies of primary rat hepatocytes on our 3D MWNT yarns, utilizing a sandwich culture configuration. The preliminary results revealed that hepatocytes were enclosed between thin layers of collagen. Through observations made and optical images taken, rat hepatocytes showed a greater tendency to attach to 6-ply yarn (see Figure 3B) than to single-ply yarns (Figure 3A).

3.3. Polarization of Primary Rat Hepatocyte on Substrates with Nanoscale Topography. We then observed the correlation between culture substrate and hepatocyte polarity, using F-actin cytoskeleton polarity as a diagnostic marker. There were significant differences between hepatocytes in monolayer culture and those in sandwich culture. In monolayer culture, hepatocytes exhibit a mesh network of stress fibers on the bottom surface of the cell; presumably, these fibers start and end at the sites where cells attach to the substrate (Figure 4A). In comparison, hepatocytes in sandwich culture exhibit F-actin localized mainly along the periphery, corresponding to cell–cell contacts or pericanalicular regions.^{29,30} There are no stress fibers, and F-actin is localized to the cell periphery, which is similar to native tissue where cells possess 3D cell-ECM and cell–cell cytoskeletal networks (Figure 4C). In addition, hepatocytes in monolayer culture appear flattened and spread out, while hepatocytes in sandwich culture formed clusters of cells that are more cuboidal in shape.

3.4. Formation of a Bile Canalicular Network. An important aspect of *in vitro* hepatocyte models is their ability to correctly polarize. By polarize, we mean produce the basolateral-apical membrane orientation required for correct drug transporter functionality. We examined this polarization using 5 (and 6)-carboxy-2',7'-dichlorofluorescein diacetate (CDFDA), a specific substrate for the MRP2 drug transport protein that is localized to the apical (canalicular) membrane of polarized hepatocytes. This was done on both control (collagen only) and nanogrooved (aligned MWNT sheets) substrates using a standard sandwich configuration. Following 5 days of culture to allow polarization to occur, 5 (and 6)-carboxy-2',7'-dichlorofluorescein (CDF) excretion into pseudocanalicular spaces was detected by hepatocytes grown in sandwich culture on both control and aligned MWNT substrates (Figure 5). Note that in unpolarized cells fluorescence is absent as CDF is not exported, so CDF excretion is direct evidence for cell polarization.^{31–33} CDF excretion was similar for cells cultured on the two substrates.

3.5. Survival of Primary Rat Hepatocyte (PRH) on Substrates with Nanoscale Topography. In order to examine whether cells grown under different culture conditions (monolayer and sandwich culture) and substrate topography exhibited differential survival, we monitored the viability of hepatocytes over 7 days in culture using the XTT assay. Hepatocytes grown in monolayer configuration on both control and test substrates (aligned MWNT sheets) showed a significant decrease in cell viability over 7 days in culture, with an approximately 40% drop in cell viability observed over the culture period (Figure 6A). Substrate topography has no significant impact on viability, with no significant difference between hepatocytes grown on both the aligned MWNT sheet and control substrates at any time point.

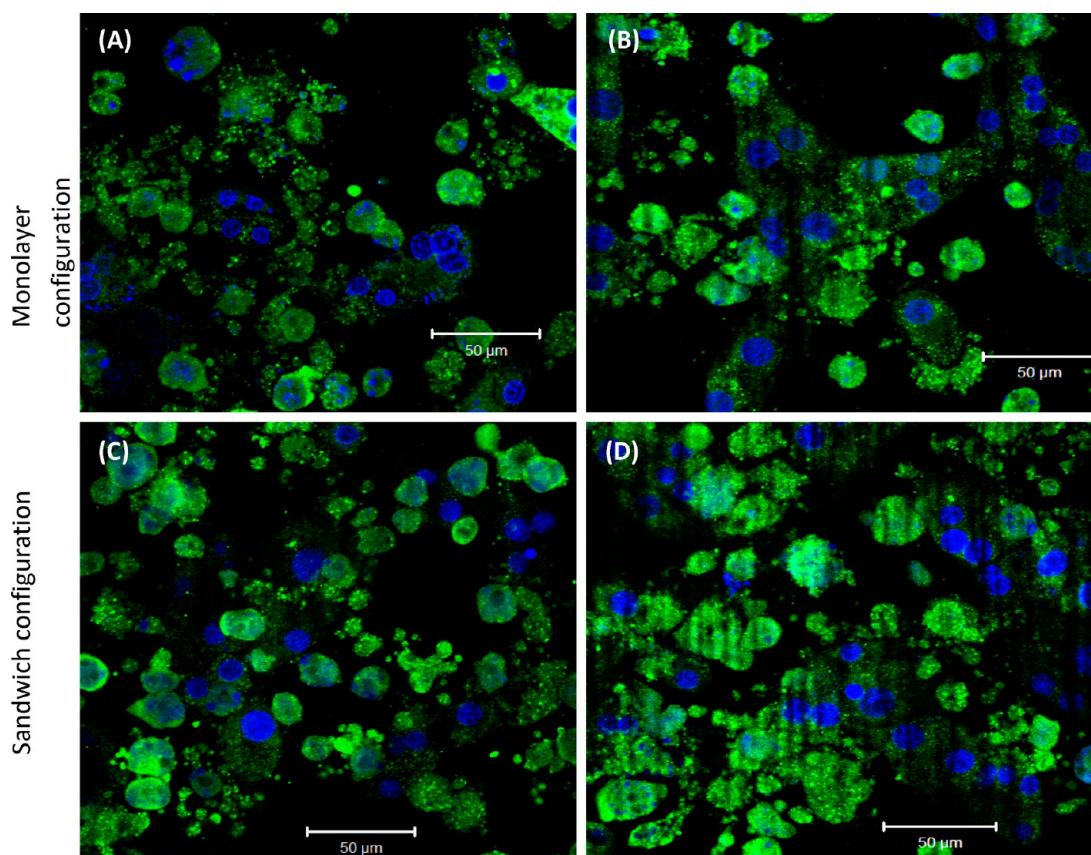


Figure 8. Representative images showed immunofluorescence staining for albumin production (green) in primary rat hepatocytes after 3 days in culture for both monolayer (A and B) and sandwich configuration (C and D). The images were obtained by confocal laser microscopy. Cell nuclei are stained with DRAQ5 (blue). The left-hand images (A and C) are of hepatocytes on control surfaces, and the right-hand images (B and D) are of hepatocytes on aligned MWNT sheets.

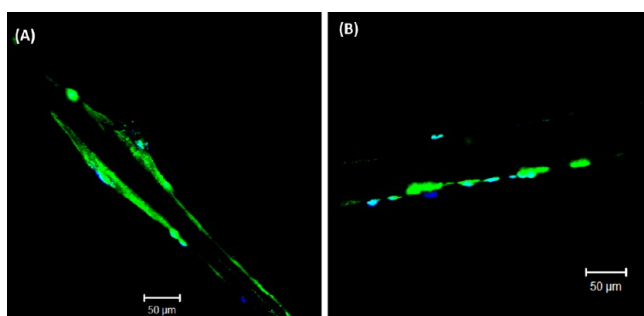


Figure 9. Representative images of immunofluorescence staining for albumin production (green) in primary rat hepatocytes cultured between thin layers of collagen on (A) single-ply yarn and (B) 6-ply yarn. DRAQ5 stains the nuclei blue.

Hepatocytes in sandwich culture exhibited improved maintenance of cell viability over time on both substrates, with only an approximately 25% decrease in viability observed over the observation period (Figure 6B). The results of this study indicated no significant difference between the two substrates at three different time periods. The results for viability in Figure 6 are in agreement with a number of published studies, where survival is enhanced in sandwich culture.^{34–37}

3.6. Cytochrome P450 (CYP450) Enzyme Activities.

Next, we quantify the enzyme activity of the cytochrome P450 subfamily members CYP1A2 and CYP3A4 using the P450-Glo

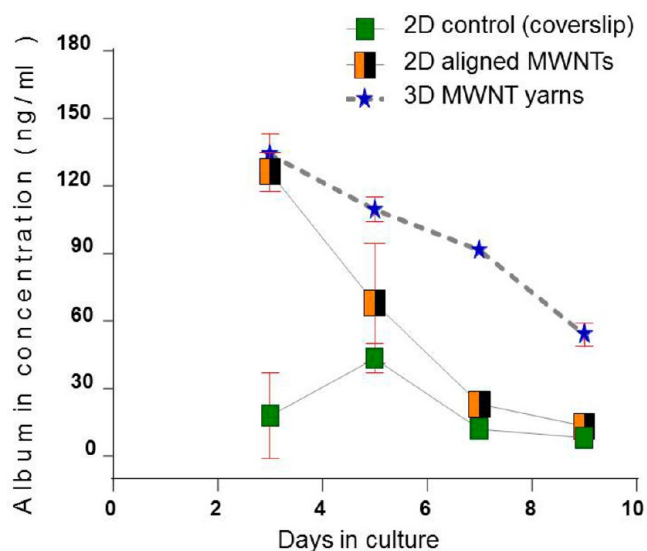


Figure 10. Amounts of albumin secreted by the rat hepatocytes in sandwich configuration on different culture systems and surfaces were determined after 3, 5, 7, and 9 days of culture. On a daily basis, medium samples were taken from the culture system. $N = 4$ from a single experiment. Error bar = standard deviation.

assay. We measured the activity in hepatocytes on both control and aligned MWNT sheet substrates. Only cells in sandwich configurations were examined, as these had previously been

shown to have superior characteristics compared to monolayer cells.

Basal activity levels for CYP1A2 and CYP3A4 were not significantly different between hepatocytes cultured on control and MWNT-sheet substrates (data not shown). However, following exposure to prototypical inducers for 48 h, activity levels of CYP1A2 but not of CYP3A4 were significantly higher in hepatocytes cultured on MWNT sheets compared to control substratum (Figure 7). In the case of CYP1A2, the fold induction over basal following induction with beta-Naphthoflavone (β -NF) for rat hepatocytes plated on MWNT-sheet surfaces was double that for coverslips, being 6.0 ± 0.4 -fold and 3.8 ± 0.2 -fold, respectively. According to an unpaired two-tailed *t* test, the fold CYP1A2 induction is significantly ($P = 0.0014$) higher on our aligned MWNTs than on coverslips. Fold induction of CYP3A4 activity in rat hepatocytes following exposure with Dex was 19% higher on MWNT-plated cells compared to control-plated cells, being 7.0 ± 0.7 and 5.9 ± 0.2 -fold, respectively. This is not significant ($P = 0.062$).

This is comparable to the findings of Rothenberg and co-workers¹⁷ on nanofiber surfaces (Ultra-Web and Ultra-Web polyamines). Following induction with dexamethasone (Dex) and pregnenolone-16 α -carbonitrile (PCN), CYP3A activity measured for hepatocytes was 5-fold higher than hepatocytes grown on collagen surfaces. Also, Wang et al.¹⁶ demonstrated higher albumin, urea secretion, and cytochrome P450 (CYP1A1) activities for hepatocytes cultured on PuraMatrix scaffold.

3.7. Qualitative and Quantitative Measurement of Albumin Synthesis of Primary Rat Hepatocyte (PRH) on Substrates with Nanoscale Topography. The secretion of albumin is used as an indicator of liver phenotypic functionality and was examined. Both monolayer-grown hepatocytes and hepatocytes in sandwich configuration produced albumin on aligned MWNT sheets (Figure 8) and yarns (Figure 9), in agreement with the findings of Wang et al.³⁸

Next, we quantitated the amount of albumin secreted: Figure 10 shows albumin secretion during the 9-day culture period in 2D and 3D culture systems. Albumin secretion into culture medium from hepatocytes grown on both test and control surfaces was detectable during the entire culture period, although the amount decreased from the beginning to the end of cell culture. Particularly at early times, the albumin secreted by rat hepatocytes on aligned MWNT sheets was significantly higher than on control substrates. The levels of albumin secretion on aligned MWNTs on days 3, 5, 7, and 9 of culture were 126 ± 9 , 68 ± 27 , 23 ± 3 , and 13 ± 2 ng/mL, respectively.

As we have XTT absorbance estimates for viable cell numbers on days 3, 5, and 7, we can estimate the albumin production per viable cell for these 3 days. The XTT and albumin measurements were separate experiments. The ratios of albumin concentration to XTT absorbance are 642, 384, and 149 for the cells on MWNT substrates on days 3, 5, and 7, respectively. For cells on the coverslips, the ratios are 88, 254, and 80 for days 3, 5, and 7, respectively. The albumin production per viable cell is significantly greater on the MWNT substrates at all times, although it decreases with time. This decrease is due to the drop in albumin production as cell viability does not vary greatly; see Figure 6.

On MWNT yarns, the secretions of albumin by rat hepatocytes on these days were 134 ± 9 , 110 ± 6 , 92 ± 1 , and 54 ± 5 ng/mL, respectively. The MWNT sheet substrates

are approximately 1 mm square, while the yarn surface area is only approximately 0.3 mm^2 , three times lower than our MWNT sheet substrates. Hence, albumin production per unit area is approximately three times higher on the 6-ply yarns, consistent with a higher level of albumin secretion per cell in our 3D yarn culture system compared to the 2D MWNT culture system. This suggests that the cells on the yarns are closer to the *in vivo* morphology; however, imaging cells on the large opaque yarns is difficult, so we could not study morphology directly. The area of 0.3 mm^2 per well is easily obtained. Each well has a single 6-ply yarn approximately $L = 2$ mm long and with diameter $D = 50 \text{ }\mu\text{m}$. The yarn is approximately cylindrical and so has a surface area equal to πLD .

4. CONCLUSIONS

To conclude, we have studied scaffolding materials whose nanoscale topography directly guides the adhesion and growth of primary hepatocytes. Our MWNT sheet substrates are able to sustain liver-specific function including albumin synthesis, Phase I (CYP 1A2/3A4) enzyme activity, and transporter activity. Upon induction with beta-Naphthoflavone (β -NF), the induction of CYP1A activity of primary rat hepatocytes on our aligned MWNT sheet substrates was approximately double that of cells on a control flat glass coverslip. Primary rat hepatocytes on MWNT-based substrates also maintain their morphology and functional activity such as cell polarity.

In the future, we will continue to explore potential uses of both 2D and 3D scaffolds for drug development applications. In particular, our yarns offer the potential to construct tough 3D scaffolds of controllable geometry. Our preliminary findings of high levels of albumin secretion by cells on our yarns suggest that these yarns provide an environment which is sufficiently *in vivo*-like to allow high levels of liver function, and in addition, these yarns are tough and can be made into almost any woven 3D structure.

■ ASSOCIATED CONTENT

📄 Supporting Information

Description of how we culture our cells and perform the required assays. This material is available free of charge via the Internet at <http://pubs.acs.org>.

■ AUTHOR INFORMATION

Corresponding Author

*E-mail: azurahamanim@upm.edu.my; azurahamanim@gmail.com.

Notes

The authors declare no competing financial interest.

■ ACKNOWLEDGMENTS

C.A.C.A. acknowledges the Malaysian Ministry of Higher Education (MOHE) and the Universiti Putra Malaysia for providing financial support for her PhD studies. We acknowledge support from the University of Surrey's EPSRC-funded Knowledge Transfer Account.

■ REFERENCES

- (1) Hawkins, M. T.; Lewis, J. H. Latest Advances in Predicting DILI in Human Subjects: Focus on Biomarkers. *Expert Opin. Drug Metab. Toxicol.* **2012**, *8*, 1521–1530.
- (2) Plant, N. Strategies for Using In Vitro Screens in Drug Metabolism. *Drug Discovery Today* **2004**, *9*, 328–336.

- (3) Gille, C.; Bolling, C.; Hoppe, A.; Bulik, S.; Hoffmann, S.; Hubner, K.; Karlstadt, A.; Ganeshan, R.; Konig, M.; Rother, K.; Weidlich, M.; Behre, J.; Holzhutter, H. G. HepatoNet1: A Comprehensive Metabolic Reconstruction of the Human Hepatocyte for the Analysis of Liver Physiology. *Mol. Syst. Biol.* **2013**, *6*, 411.
- (4) Fisher, C. P.; Plant, N. J.; Moore, J. B.; Kierzek, A. M. QSSPN: Dynamic Simulation of Molecular Interaction Networks Describing Gene Regulation, Signalling and Whole-Cell Metabolism in Human Cells. *Bioinformatics* **2013**, *29*, 3181–3190.
- (5) Pushparajah, D. S.; Umachandran, M.; Plant, K. E.; Plant, N.; Ioannides, C. Evaluation of the Precision-Cut Liver and Lung Slice Systems for the Study of Induction of CYP1, Epoxide Hydrolase and Glutathione S-transferase Activities. *Toxicology* **2007**, *231*, 68–80.
- (6) Papageorgiou, I.; Grepper, S.; Unadkat, J. D. Induction of Hepatic CYP3A Enzymes by Pregnancy-Related Hormones: Studies in Human Hepatocytes and Hepatic Cell Lines. *Drug Metab. Dispos.* **2013**, *41*, 281–290.
- (7) Schaefer, O.; Ohtsuki, S.; Kawakami, H.; Inoue, T.; Liehner, S.; Saito, A.; Sakamoto, A.; Ishiguro, N.; Matsumaru, T.; Terasaki, T.; Ebner, T. Absolute Quantification and Differential Expression of Drug Transporters, Cytochrome P450 Enzymes, and UDP-Glucuronosyltransferases in Cultured Primary Human Hepatocytes. *Drug Metab. Dispos.* **2012**, *40*, 93–103.
- (8) Li, N.; Singh, P.; Mandrell, K. M.; Lai, Y. Improved Extrapolation of Hepatobiliary Clearance from In Vitro Sandwich Cultured Rat Hepatocytes Through Absolute Quantification of Hepatobiliary Transporters. *Mol. Pharm.* **2010**, *7*, 630–641.
- (9) Howe, K.; Gibson, G. G.; Coleman, T.; Plant, N. In Silico and In Vitro Modeling of Hepatocyte Drug Transport Processes: Importance of ABCC2 Expression Levels in the Disposition of Carboxydichlorofluorescein. *Drug Metab. Dispos.* **2009**, *37*, 391–399.
- (10) Wang, Y. J.; Liu, H. L.; Guo, H. T.; Wen, H. W.; Liu, J. Primary Hepatocyte Culture in Collagen Gel Mixture and Collagen Sandwich. *World J. Gastroenterol.* **2004**, *10*, 699–702.
- (11) Kono, Y.; Roberts, E. A. Modulation of the Expression of Liver-Specific Functions in Novel Human Hepatocyte Lines Cultured in a Collagen Gel Sandwich Configuration. *Biochem. Biophys. Res. Commun.* **1996**, *220*, 628–632.
- (12) Berry, C. C.; Campbell, G.; Spadicino, A.; Robertson, M.; Curtis, A. S. The Influence of Microscale Topography on Fibroblast Attachment and Motility. *Biomaterials* **2004**, *25*, 5781–5788.
- (13) Khademhosseini, A.; Langer, R.; Borenstein, J.; Vacanti, J. P. Microscale Technologies for Tissue Engineering and Biology. *Proc. Natl. Acad. Sci. U. S. A.* **2006**, *103*, 2480–2487.
- (14) Charest, J. L.; Garcia, A. J.; King, W. P. Myoblast Alignment and Differentiation on Cell Culture Substrates with Microscale Topography and Model Chemistries. *Biomaterials* **2007**, *28*, 2202–2210.
- (15) Zhang, S.; Xia, L.; Kang, C. H.; Xiao, G.; Ong, S. M.; Toh, Y. C.; Leo, H. L.; van Noort, D.; Kan, S. H.; Tang, H. H.; Yu, H. Microfabricated Silicon Nitride Membranes for Hepatocyte Sandwich Culture. *Biomaterials* **2008**, *29*, 3993–4002.
- (16) Wang, S.; Nagrath, D.; Chen, P. C.; Berthiaume, F.; Yarmush, M. L. Three-Dimensional Primary Hepatocyte Culture in Synthetic Self-Assembling Peptide Hydrogel. *Tissue Eng. Part A* **2008**, *14*, 227–236.
- (17) Rothenberg, M. E.; Cali, J. J.; Sobol, M.; Briggs, M. W.; Upton, T. Rat Hepatocyte Culture Physiology Shows Enhanced Cytochrome P450 Activity on a Synthetic Extracellular Matrix. *In Vitro Toxicol.* **2008**, *1*, 18–20.
- (18) Wang, L.; Carrier, R. L. Biomimetic Topography: Bioinspired Cell Culture Substrates and Scaffolds. In *Advances in Biomimetics*; George, A., Ed.; InTech: Rijeka, Croatia, 2011; Chapter 21, pp 453–472.
- (19) Tsai, W. B.; Lin, J. H. Modulation of Morphology and Functions of Human Hepatoblastoma Cells by Nano-Grooved Substrata. *Acta Biomater.* **2009**, *5*, 1442–1454.
- (20) Bettinger, C. J. Synthesis and Microfabrication of Biomaterials for Soft-Tissue Engineering. *Pure Appl. Chem.* **2009**, *81*, 2183–2201.
- (21) Zhang, M.; Fang, S.; Zakhidov, A. A.; Lee, S. B.; Aliev, A. E.; Williams, C. D.; Atkinson, K. R.; Baughman, R. H. Strong, Transparent, Multifunctional, Carbon Nanotube Sheets. *Science* **2005**, *309*, 1215–1219.
- (22) Atkinson, K. R.; Hawkins, S. C.; Huynh, C.; Skourtis, C.; Dai, J.; Zhang, M.; Fang, S.; Zakhidov, A. A.; Lee, S. B.; Aliev, A. E.; Williams, C. D.; Baughman, R. H. Multifunctional Carbon Nanotube Yarns and Transparent Sheets: Fabrication, Properties, and Applications. *Phys. B* **2007**, *394*, 339–343.
- (23) Zhang, M.; Atkinson, K. R.; Baughman, R. H. Multifunctional Carbon Nanotube Yarns by Downsizing an Ancient Technology. *Science* **2004**, *306*, 1358–1361.
- (24) Abdullah, C. A.; Asanithi, P.; Brunner, E. W.; Jurewicz, I.; Bo, C.; Azad, C. L.; Ovalle-Robles, R.; Fang, S.; Lima, M. D.; Lepro, X.; Collins, S.; Baughman, R. H.; Sear, R. P.; Dalton, A. B. Aligned, Isotropic and Patterned Carbon Nanotube Substrates that Control the Growth and Alignment of Chinese Hamster Ovary Cells. *Nanotechnology* **2011**, *22*, 205102.
- (25) Pavese, M. M. S.; Bianco, S.; Giorcelli, M.; Pugno, N. An Analysis of Carbon Nanotube Structure Wettability Before and After Oxidation Treatment. *J. Phys.: Condens. Matter* **2008**, *20*, 474206.
- (26) Duncan, A. W. Aneuploidy, polyploidy and ploidy reversal in the liver. *Semin. Cell Dev. Biol.* **2013**, *24*, 347–356.
- (27) Le Guilly, Y.; Lenoir, P.; Bourel, M. Production of Plasma Proteins by Subcultures of Adult Human Liver. *Biomedicine* **1973**, *19*, 361–364.
- (28) Mooney, D.; Hansen, L.; Vacanti, J.; Langer, R.; Farmer, S.; Ingber, D. Switching from Differentiation to Growth in Hepatocytes: Control by Extracellular Matrix. *J. Cell Physiol.* **1992**, *151*, 497–505.
- (29) Ranucci, C. S.; Kumar, A.; Batra, S. P.; Moghe, P. V. Control of Hepatocyte Function on Collagen Foams: Sizing Matrix Pores Toward Selective Induction of 2-D and 3-D Cellular Morphogenesis. *Biomaterials* **2000**, *21*, 783–793.
- (30) Ezzell, R. M.; Toner, M.; Hendricks, K.; Dunn, J. C.; Tompkins, R. G.; Yarmush, M. L. Effect of Collagen Gel Configuration on the Cytoskeleton in Cultured Rat Hepatocytes. *Exp. Cell Res.* **1993**, *208*, 442–452.
- (31) Bow, D. A. J.; Perry, J. L.; Miller, D. S.; Pritchard, J. B.; Brouwer, K. L. R. Localization of P-gp (Abcb1) and Mrp2 (Abcc2) in Freshly Isolated Rat Hepatocytes. *Drug Metab. Dispos.* **2008**, *36*, 198–202.
- (32) Howe, K.; Gibson, G. G.; Coleman, T.; Plant, N. In Silico and In Vitro Modeling of Hepatocyte Drug Transport Processes: Importance of ABCC2 Expression Levels in the Disposition of Carboxydichlorofluorescein. *Drug Metab. Dispos.* **2009**, *37*, 391–399.
- (33) Tian, X.; Zamek-Gliszczynski, M. J.; Zhang, P.; Brouwer, K. L. R. Modulation of Multidrug Resistance-Associated Protein 2 (Mrp2) and Mrp3 Expression and Function with Small Interfering RNA in Sandwich-Cultured Rat Hepatocytes. *Mol. Pharmacol.* **2004**, *66*, 1004–1010.
- (34) Richert, L.; Binda, D.; Hamilton, G.; Viollon-Abadie, C.; Alexandre, E.; Bigot-Lasserre, D.; Bars, R.; Coassolo, P.; LeCluyse, E. Evaluation of the Effect of Culture Configuration on Morphology, Survival Time, Antioxidant Status and Metabolic Capacities of Cultured Rat Hepatocytes. *Toxicol. In Vitro* **2002**, *16*, 89–99.
- (35) LeCluyse, E. L.; Bullock, P. L.; Parkinson, A. Strategies for Restoration and Maintenance of Normal Hepatic Structure and Function in Long-term Cultures of Rat Hepatocytes. *Adv. Drug Delivery Rev.* **1996**, *22*, 133–186.
- (36) Schutte, M.; Fox, B.; Baradez, M. O.; Devonshire, A.; Minguéz, J.; Bokhari, M.; Przyborski, S.; Marshall, D. Rat Primary Hepatocytes Show Enhanced Performance and Sensitivity to Acetaminophen During Three-Dimensional Culture on a Polystyrene Scaffold Designed for Routine Use. *Assay Drug Dev. Technol.* **2011**, *9*, 475–486.
- (37) Dunn, J. C.; Yarmush, M. L.; Koebe, H. G.; Tompkins, R. G. Hepatocyte Function and Extracellular Matrix Geometry: Long-Term Culture in a Sandwich Configuration. *FASEB J.* **1989**, *3*, 174–177.
- (38) Wang, A.; Xia, T.; Ran, P.; Chen, X.; Nuessler, A. K. Qualitative Study of Three Cell Culture Methods. *J. Huazhong Univ. Sci. Technol., Med. Sci.* **2002**, *22*, 288–291.